



RESEARCH LETTER

10.1002/2017GL073519

Key Points:

- ACE-FTS observes extreme concentrations of HCN in lower stratosphere in 2016
- HCN concentrations in the lower stratosphere are the largest values on record
- Enhancements linked to El Niño-driven high temperatures, drought in Southeast Asia

Correspondence to:

K. A. Walker,
kaley.walker@utoronto.ca

Citation:

Sheese, P. E., K. A. Walker, and C. D. Boone (2017), A global enhancement of hydrogen cyanide in the lower stratosphere throughout 2016, *Geophys. Res. Lett.*, *44*, 5791–5797, doi:10.1002/2017GL073519.

Received 18 MAR 2017

Accepted 18 MAY 2017

Accepted article online 22 MAY 2017

Published online 11 JUN 2016

A global enhancement of hydrogen cyanide in the lower stratosphere throughout 2016

Patrick E. Sheese¹, Kaley A. Walker¹, and Chris D. Boone²

¹Department of Physics, University of Toronto, Toronto, Ontario, Canada, ²Department of Chemistry, University of Waterloo, Waterloo, Ontario, Canada

Abstract In September–October 2015, El Niño-driven weather conditions led to one of the most intense Indonesian peatland burning events in recent history. Consequently, an unprecedented amount of hydrogen cyanide (HCN) was emitted from Southeast Asia and transported into the upper troposphere and lower stratosphere, which was then transported by the general circulation from the tropics to polar latitudes. By early 2016, the daily mean concentrations of HCN in the lower stratosphere at all latitudes, as measured by the Atmospheric Chemistry Experiment Fourier Transform Spectrometer (ACE-FTS) instrument, were the largest on record for the region, on the order of 40–90% greater than the climatological mean and ~40% greater than the 2007 El Niño-driven values. By December 2016, levels of polar HCN in the lower stratosphere were still on the order 10–20% greater than the climatological mean. These ACE-FTS measurements are thus vital for interpreting ground-based and nadir satellite measurements of HCN made during 2016 and could be used to help validate tropospheric-stratospheric exchange in climate models.

1. Introduction

El Niño is a climate phenomenon that is predominantly defined by prolonged above-average sea surface temperatures in the equatorial Pacific Ocean. One predictable consequence of these high sea surface temperatures is an increase in atmospheric surface temperatures and a decrease in precipitation in Southeast Asia. In the mainland Southeast Asia region, seasonal biomass burning occurs near the end of each Northern Hemisphere (NH) winter, typically peaking around March, in part due to local agricultural practices. In Indonesia, a similar biomass burning season occurs each winter in the Southern Hemisphere, typically peaking around September–October. In years with strong El Niño conditions, these biomass burning events can be exacerbated by the accompanying high temperatures and drought conditions [Field *et al.*, 2009]. As well, in Indonesia, much of the peatlands have been deforested, leaving them drier and more prone to catching fire. In September and October of 2015, in the middle of a pronounced El Niño event, Indonesian peatland fires were the largest they had been, in terms of emitted carbon and burnt area [Parker *et al.*, 2016; Huijnen *et al.*, 2016; Field *et al.*, 2016], since the similar Indonesian biomass burning event in 1997, emitting large amounts of hydrogen cyanide (HCN) into the lower stratosphere. In 1997–1998, as shown by Rinsland *et al.* [1999, 2000], tropospheric partial column HCN concentrations in the NH were a factor of 2–3 times greater than the climatological mean.

In 2016, as shown by National Oceanic and Atmospheric Administration National Centers for Environmental Information temperature and precipitation anomaly data available at <https://www.ncdc.noaa.gov> and as reported by multiple media outlets (e.g., CNN, 2016, <http://www.cnn.com/2016/05/12/homepage2/southeast-asia-drought-el-nino/>, last accessed 17 Feb 2017), the mainland Southeast Asia region suffered from severe drought and many countries in the region, including Thailand and Cambodia, reported record-setting high temperatures. As is shown in this study, the 2016 mainland Southeast Asia burning season extended well into April and was the most intense in over a decade, further contributing to elevated levels of HCN in the upper troposphere-lower stratosphere (UTLS) throughout the year.

HCN is a tropospheric pollutant that is released into the atmosphere predominantly through biomass burning, especially in the burning of peat, and also in industrial activities. The burning of peat is known to emit roughly 5–10 times more HCN than the burning of other typical biomass products [Christian *et al.*, 2003; Akagi *et al.*, 2011]. The ACE-FTS (Atmospheric Chemistry Experiment Fourier Transform Spectrometer) instrument [Bernath *et al.*, 2005] is the only satellite limb sounder that currently measures vertically resolved profiles of HCN in the UTLS. The ACE-FTS HCN data have been used extensively, e.g., by Randel *et al.* [2010] in identifying the Asian monsoon anticyclone (AMA) as a vehicle for transporting tropospheric pollution to the stratosphere, by Pumphrey *et al.* [2008] and Pommrich *et al.* [2010] in

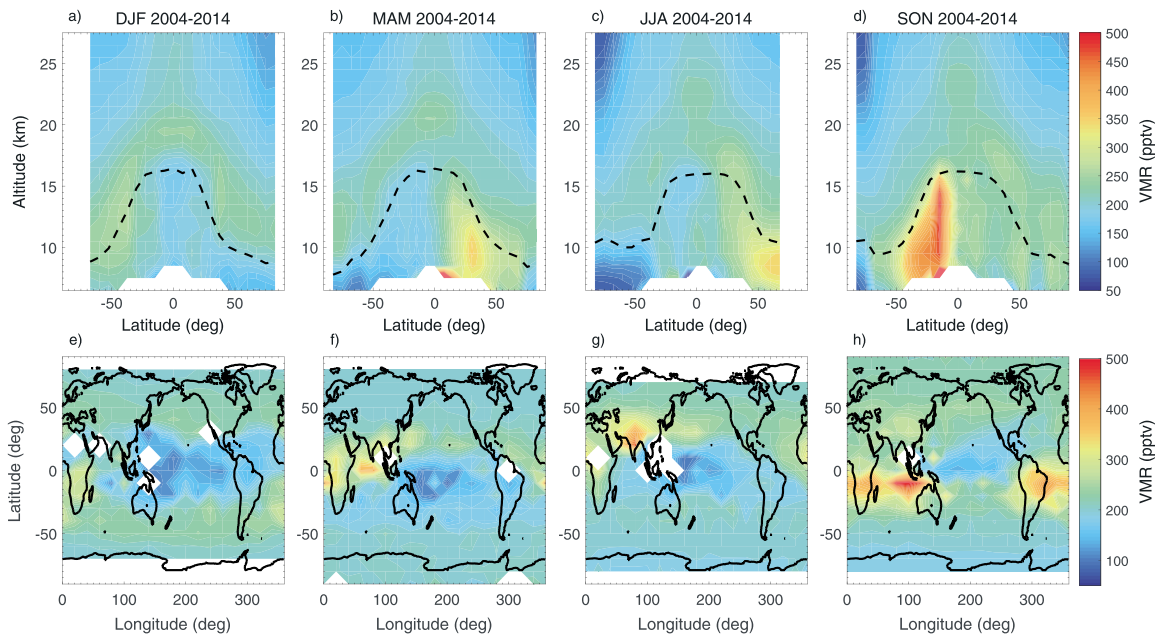


Figure 1. The top row shows latitudinal cross section of 2004–2014 zonal mean ACE-FTS HCN climatologies in 5° latitude and 1 km altitude bins for (a) December–February, (b) March–May, (c) June–August, and (d) September–November. The dashed lines indicate the height of the calculated climatological tropopause. The bottom row shows global 2004–2014 HCN climatologies in 10° latitude and 20° longitude bins at an altitude of 14.5 km for (e) December–February, (f) March–May, (g) June–August, and (h) September–November.

identifying and investigating the HCN tropical “tape recorder” signal, and by *Li et al.* [2009] and *Glatthor et al.* [2015] in measuring HCN variations in the upper troposphere and stratosphere.

2. ACE-FTS HCN Measurements

ACE-FTS is a solar occultation instrument measuring in the infrared between 750 and 4400 cm^{-1} with 0.02 cm^{-1} spectral resolution. The HCN retrievals, detailed by *Boone et al.* [2005, 2013], extend from 6 km to 42 km with a vertical resolution on the order of 3–6 km, depending on the viewing geometry. ACE-FTS version 3.5/3.6 HCN data were used in this study. Pre-March 2013 is typically v3.5, and post-March 2013 data (as well as ~5% of the pre-March 2013 data) were processed using the same technique and algorithm as v3.5 [*Boone et al.*, 2013] except were processed on a supercomputing network (v3.6) instead of a local network. An analysis of reprocessed v3.5 data showed no significant differences between the original v3.5 HCN data and HCN data reprocessed on the supercomputing network. To screen the data for unphysical outliers, version 2.0 of the ACE-FTS data quality flags [*Sheese et al.*, 2015] was used. It should be noted that ~8% of HCN profiles that were originally flagged as containing outlying data were included in the analysis, as they were found to be highly correlated (correlation coefficient greater than 0.95) with simultaneously observed ACE-FTS CO profiles. Both HCN and CO are long-lived tracers of biomass burning.

Figures 1a–1d show the seasonal ACE-FTS 2004–2014 HCN zonal mean climatologies in 5° latitude and 1 km altitude bins, as well as calculated climatological tropopause heights (World Meteorological Organization lapse-rate definition [*World Meteorological Organization*, 1957]). Figures 1e–1h show similar global seasonal 2004–2014 HCN climatologies at 14.5 km in 10° latitude and 20° longitude bins. *Glatthor et al.* [2015] discussed HCN seasonal variations in the UTLS in terms of MIPAS (Michelson Interferometer for Passive Atmospheric Sounding) observations. The MIPAS HCN climatology [*Glatthor et al.*, 2015, Figure 2] qualitatively agrees well with that of ACE-FTS. The December–February season (ACE-FTS shown in Figure 1a) in both data sets exhibits the lowest tropospheric HCN values throughout the year and a layer of HCN in the lower stratosphere that extends to higher latitudes. In the March–May (MAM) season, shown in Figure 1b, HCN enhancements are observed in the northern tropics to midlatitudes in the upper troposphere, attributable, as seen in Figure 1f, to biomass burning in tropical Africa and Southeast Asia [*Hsu et al.*, 2003; *van der Werf et al.*, 2010]. The June–August (JJA) season (Figure 1c) in both ACE-FTS and MIPAS data sets exhibits enhancement in the

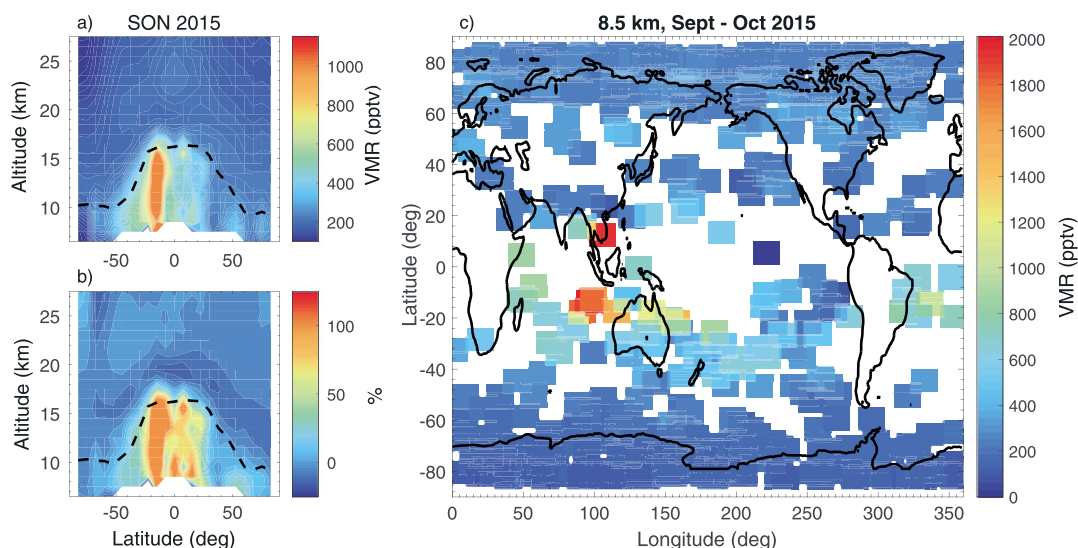


Figure 2. (a) Latitudinal cross section of zonal mean HCN profiles for September–November (SON) 2015 and (b) latitudinal cross sections of percent deviations of SON 2015 zonal mean HCN from the 2004–2014 climatological means in 5° latitude and 1 km altitude bins. (c) Global map of HCN at 8.5 km for 1 September to 4 November 2015 with measurements smoothed by 10° latitude and 20° longitude running mean.

northern midlatitude to high latitude in the upper troposphere, with the midlatitude enhancement, which is due to the AMA transporting pollution from the lower troposphere (Figure 1g), extending up into the stratosphere near 18 km [Randel *et al.*, 2010; Park *et al.*, 2013]. Both data sets show yearly peak HCN values during the September–November (SON) season (Figure 1d) in the southern tropics to midlatitudes in the upper troposphere. As shown in Figure 1h, this is attributable to intense biomass burning in Africa, South America, and Indonesia [Edwards *et al.*, 2006; Pommrich *et al.*, 2010]. Additional enhancements in the NH UTLS are probably the remainder of the summer HCN enhancement transported up from the AMA. As seen in Figures 1e–1h, at low latitudes in the upper troposphere, during all seasons, there is a HCN minimum above the tropical Pacific Ocean, which is the predominant sink of HCN [Li *et al.*, 2003; Singh *et al.*, 2003].

3. HCN Enhancements in 2016

Figure 2a shows zonally averaged SON 2015 data in 5° latitude and 1 km altitude bins, and Figure 2b shows the percent deviation of the data in Figure 2a from the SON 2004–2014 climatological mean. The ACE-FTS data exhibit enhancements of HCN in the upper troposphere in the southern tropics to midlatitudes and northern tropics, with zonally averaged concentrations of over 1 ppbv (parts per billion by volume), corresponding to more than double the climatological mean. The corresponding global map of HCN during September and October 2015 at 8.5 km (Figure 2c) shows that this enhancement was mainly situated above the Indonesian region, with concentrations reaching over 2 ppbv at this altitude. HCN was then transported up into the lower stratosphere by early 2016, as shown in Figure 3. Figures 3a–3d show similar plots to Figure 2a but for seasons from winter 2015/2016 to autumn 2016, and Figures 3e–3h show the corresponding percent deviations of the zonal seasonal means from the 2004–2014 climatological means. The enhanced layer in the lower stratosphere is then further diluted and transported to all latitudes sampled by ACE-FTS in the MAM season. During this time there is another tropospheric enhancement, which is in part due to biomass burning in Southeast Asia, as discussed below. The enhanced lower stratospheric HCN layer persists throughout the 2016 JJA and SON seasons at all sampled latitudes. Figure 4 shows monthly total fire radiative power (FRP) values from the CAMS GFAS (Copernicus Atmosphere Monitoring Service Global Fire Assimilation System) for two different geographical areas—Indonesia (10°S – 5°N ; 90° – 150°E) and mainland South Asia (10° – 30°N ; 60° – 90°E). The total FRP data [Kaiser *et al.*, 2012] can be used as a proxy for fire intensity and biomass consumption rates [Wooster *et al.*, 2005] and were obtained from <http://eccharts.ecmwf.int/datasets/data/cams-gfas>. The Indonesian FRP data (Figure 4a) show that the 2015 biomass burning season, peaking in October, was by far the most intense of all years since 2004. Previous to 2015, the biomass burning

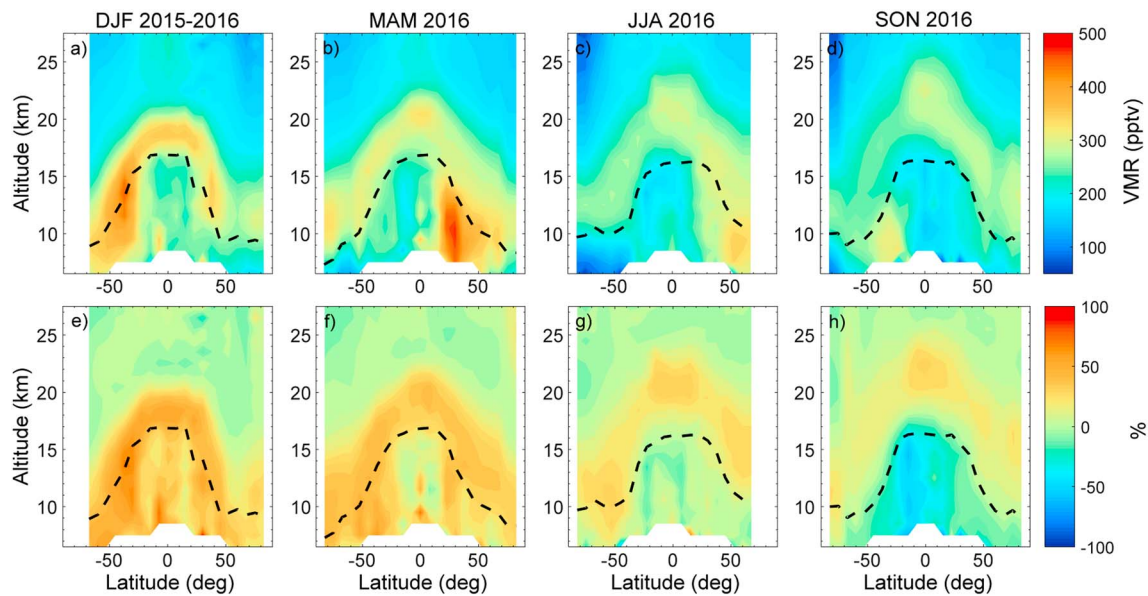


Figure 3. (a–d) Seasonal latitudinal cross sections of zonal mean HCN profiles for December 2015 to November 2016. (e–h) Latitudinal cross sections of percent deviations of seasonal zonal mean HCN from the 2004–2014 climatological means. From left to right, December 2015–February 2016, March–May 2016, June–August 2016, and September–November 2016. Data are averaged in 5° latitude and 1 km altitude bins.

of 2006 was the most intense. The FRP data for the Southeast Asia region (Figure 4b) show that the April 2016 values were the greatest April values recorded for the duration of the ACE-FTS mission.

In order to get a better understanding of the evolution of HCN in the UTLS over time, Figures 5a–5c show the time series of daily-mean HCN profiles from October 2015 to October 2016 for the latitude bands 50–90°N, 35°S–35°N, and 50–90°S. In October 2015, in the low latitudes (Figure 5b) HCN concentrations were on average 490 parts per trillion by volume (pptv) in the upper troposphere, which is on the order of 100–130% greater than the climatological mean. This is in agreement with *Rinsland et al.* [1999, 2000], who showed that in 1998, following the intense El Niño-driven wild fires in Indonesia, HCN tropospheric partial column densities throughout the NH were greater than double typical values. In October and November 2015 in this region, lower stratospheric HCN values were typically within 1σ from the climatological mean.

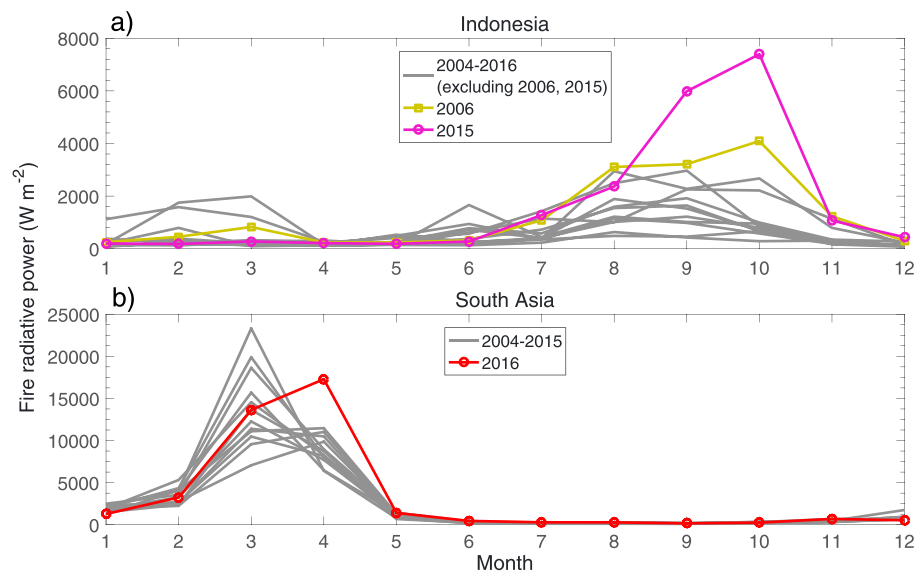


Figure 4. Monthly total fire radiative power from CAMS GFAS (Copernicus Atmosphere Monitoring Service Global Fire Assimilation System) for 2004–2106 in (a) Indonesia (10°S–5°N; 90–150°E) and (b) mainland South Asia (10–30°N; 60–90°E).

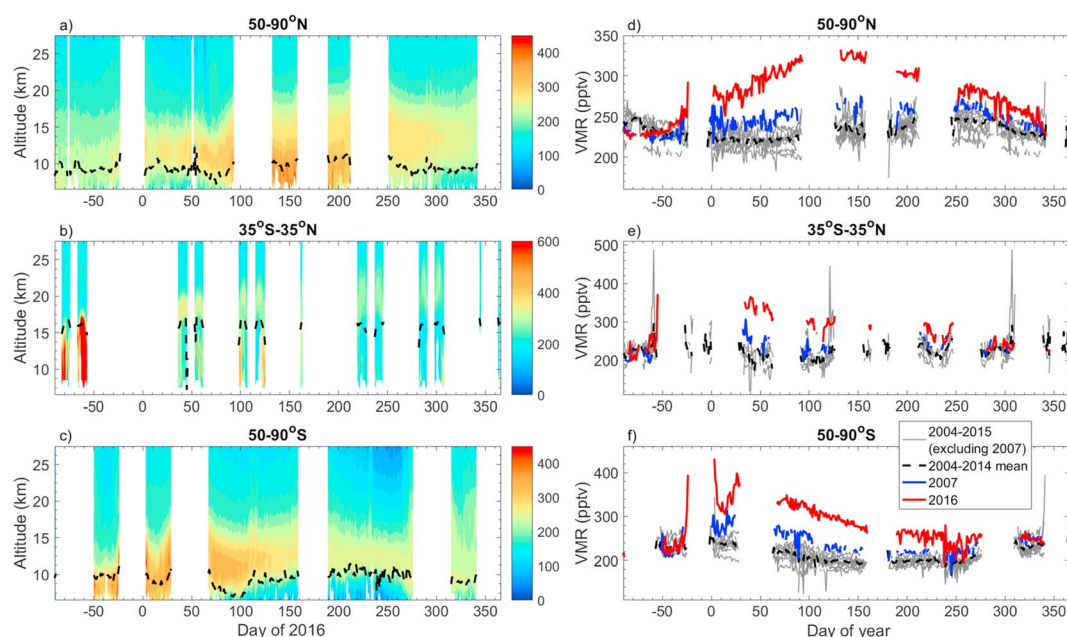


Figure 5. (a–c) Daily-mean HCN profile time series from September 2015 to September 2016. (d–f) Daily-mean HCN values interpolated to 2 km above the tropopause for each year between 2004 and 2016 (solid lines), as well as the 2004–2014 mean (black, dashed line). From top to bottom daily-mean values include all data within latitude bands 50–90°N, 35°S–35°N, and 50–90°S. Note that the range of the color scale for Figure 5b is wider than for Figures 5a or 5c.

In November, shortly after the intense biomass burning season in Indonesia, ACE-FTS measurements of HCN concentrations in the high Northern latitudes (Figure 5a) were still on par with the climatological mean values at all altitudes; however, in the Southern high latitudes (Figure 5c), HCN values were on average 300–350 pptv just at and below the tropopause, which is on the order of 40–60% greater than climatological values.

By January 2016 and into early February, HCN volume mixing ratios in the southern high latitudes were greater in the lower stratosphere (~345 pptv) than in the upper troposphere (~320 pptv). By February, in the low latitudes and the northern high latitudes, there is a HCN layer just above the tropopause that has a peak value of ~350 pptv near 19 km and ~295 pptv near 12 km, respectively. A similar layer is observed in the southern high latitudes throughout March to June, with peak values decreasing from ~340 pptv to ~280 pptv. Enhancements in the upper troposphere are exhibited throughout April (days 100–126) in the 35°S–35°N latitude range. These enhancements are then extended into the high Northern latitudes in the UTLS in May, which is in line with the FRP data from GFAS shown in Figure 4b.

The 2016 HCN enhancements in the lower stratosphere were not only greater than the climatological means, but they were the largest stratospheric HCN concentrations ACE-FTS has ever measured. Figures 5d–5f show the time series of daily-mean HCN concentrations interpolated to 2 km above the calculated tropopause height for each year from 2004 to 2016. In 2016, the HCN values above the tropopause were consistently significantly larger than all other years in the ACE-FTS measurements. Previously, the 2007 values, following the El Niño-enhanced Indonesian fires in late 2006 [Field and Shen, 2008], were the largest in the ACE-FTS record. In the northern high latitudes (Figure 5d), starting at the beginning of November 2015 and continuing to the beginning of April, HCN concentrations 2 km above the tropopause increased from on the order of the climatological mean to 45% greater than the climatological mean and up to 32% greater than the 2007 values. In the southern high latitudes (Figure 5f), the 2016 lower stratospheric values increased from on the order of the climatological mean to 82% greater than the climatological mean at the end of January and ~42% greater by early June (60% and ~22%, respectively, greater than 2007 values). Throughout February to early May, the 2016 concentrations were 42–90% greater than the climatological values in the low latitudes (Figure 5e) and 11–63% greater than the 2007 values. By November, the 2016 HCN concentrations at 2 km above the tropopause in the northern high latitudes were still typically greater than all previous years, on average 11% greater than the climatological mean. However, in the southern high latitudes and the

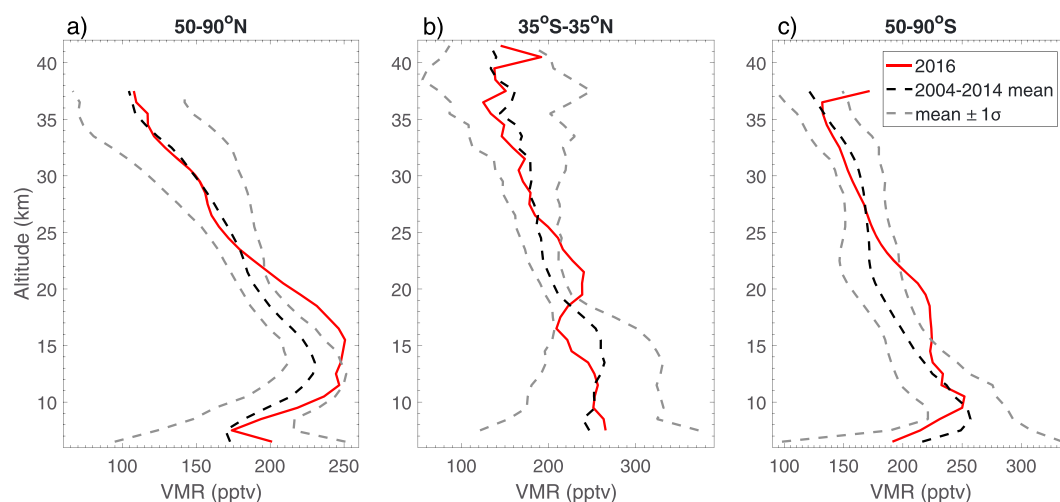


Figure 6. Average December 2016 HCN profiles with 2004–2014 climatological mean profiles and the $\pm 1\sigma$ standard deviation values for latitude bands (a) 50–90°N, (b) 35°S–35°N, and (c) 50–90°S.

low latitudes, the November 2016 values were on the same order of the climatological mean. Although, HCN enhancements are observed at higher altitudes in the stratosphere.

Figure 6 shows the mean December 2016 HCN profiles as well as the 2004–2014 mean December profiles and the $\pm 1\sigma$ values for the latitude bands 50–90°N, 35°S–35°N, and 50–90°S. In all three latitude bands, enhancements of HCN near ~20 km are still observed, greater than the 2004–2014 climatological mean + 1σ . In December 2016, HCN values were still 12–16% above climatological mean values between 15 and 20 km in the high Northern latitudes, 10–21% above climatological mean values between 20 and 24 km in the low latitudes, and 11–21% above climatological mean values between 16 and 22 km in the high Southern latitudes.

4. Summary

The indirect effects of strong El Niño conditions at the surface on global HCN concentrations in the UTLS have been observed using measurements from the ACE-FTS satellite instrument. The extreme El Niño conditions of 2015–2016 brought high temperatures and drought conditions to Southeast Asia. These conditions exacerbated the seasonal peatland fires in Indonesia throughout September and October 2015 and led to the most intense springtime biomass burning season, especially during April 2016, in mainland Southeast Asia of the past decade. These two events were the principal sources of large concentrations of HCN in the troposphere that were eventually transported into the lower stratosphere. Consequently, there was an extreme enhancement of the HCN layer just above the tropopause at all latitudes throughout 2016. HCN concentrations at peak altitudes in the lower stratosphere increased to ~350–450 pptv in early 2016, which is on the order of 40–90% greater than the climatological mean and ~30–60% greater than the largest values previously measured by ACE-FTS. By October 2016, 1 year after the intense Indonesian fires, peak daily-mean HCN values were on the order of 260–300 pptv, consistently greater than all other daily-mean October HCN values in the ACE-FTS record. By December 2016, HCN values were still enhanced, on the order of 10–20% greater than the climatological mean, in the lower stratosphere, near 20 km. These results show that El Niño conditions can ultimately have extreme effects on the HCN budget in the lower stratosphere, which can last for a timescale of over a year.

The UTLS profiles of HCN from ACE-FTS during this 2016 enhancement provide important context for ground-based and nadir satellite measurements [e.g., *Viatte et al.*, 2014; *Duflot et al.*, 2013]. These measurements of HCN total columns, partial columns, and profiles typically rely on having accurate a priori HCN profiles; thus, the ACE-FTS measurements are crucial for these other HCN measurements throughout 2016. As well, given the relatively long lifetime of HCN in the UTLS, on the order of months to years, these measurements can be used as a case study for testing troposphere-stratosphere exchange within climate chemistry models.

Acknowledgments

This project was funded by the Canadian Space Agency (CSA). The Atmospheric Chemistry Experiment is a Canadian-led mission mainly supported by the CSA. The ACE-FTS Level 2 HCN data used in this study can be obtained via the ACE-FTS website (registration required), <http://www.ace.uwaterloo.ca>, or upon request from the corresponding author (kaley.walker@utoronto.ca). The CAMS GFAS data are publicly available via <http://eccharts.ecmwf.int/datasets/data/cams-gfas> (registration required).

References

- Akagi, S. K., R. J. Yokelson, C. Wiedinmyer, M. J. Alvarado, J. S. Reid, T. Karl, J. D. Crouse, and P. O. Wennberg (2011), Emission factors for open and domestic biomass burning for use in atmospheric models, *Atmos. Chem. Phys.*, *11*, 4039–4072, doi:10.5194/acp-11-4039-2011.
- Bernath, P. F., et al. (2005), Atmospheric Chemistry Experiment (ACE): Mission overview, *Geophys. Res. Lett.*, *32*, L15501, doi:10.1029/2005GL022386.
- Boone, C. D., R. Nassar, K. A. Walker, Y. Rochon, S. D. McLeod, C. P. Rinsland, and P. F. Bernath (2005), Retrievals for the Atmospheric Chemistry Experiment Fourier-Transform Spectrometer, *Appl. Opt.*, *44*, 7218–7231, doi:10.1364/AO.44.007218.
- Boone, C. D., K. A. Walker, and P. F. Bernath (2013), *Version 3 Retrievals for the Atmospheric Chemistry Experiment Fourier Transform Spectrometer (ACE-FTS)*, the *Atmospheric Chemistry Experiment ACE at 10: A Solar Occultation Anthology*, pp. 103–127, A. Deepak Publishing, Hampton, Va.
- Christian, T. J., B. Kleiss, R. J. Yokelson, R. Holzinger, P. J. Crutzen, W. M. Hao, B. H. Saharjo, and D. E. Ward (2003), Comprehensive laboratory measurements of biomass-burning emissions: 1. Emissions from Indonesian, African, and other fuels, *J. Geophys. Res.*, *108*(D23), 4719, doi:10.1029/2003JD003704.
- Dufлот, V., D. Hurtmans, L. Clarisse, Y. R'honi, C. Vigouroux, M. De Mazière, E. Mahieu, C. Servais, C. Clerbaux, and P.-F. Coheur (2013), Measurements of hydrogen cyanide (HCN) and acetylene (C₂H₂) from the Infrared Atmospheric Sounding Interferometer (IASI), *Atmos. Meas. Tech.*, *6*, 917–925, doi:10.5194/amt-6-917-2013.
- Edwards, D. P., et al. (2006), Satellite observed pollution from Southern Hemisphere biomass burning, *J. Geophys. Res.*, *111*, D14312, doi:10.1029/2005JD006655.
- Field, R. D., and S. S. P. Shen (2008), Predictability of carbon emissions from biomass burning in Indonesia from 1997 to 2006, *J. Geophys. Res.*, *113*, G04024, doi:10.1029/2008JG000694.
- Field, R. D., G. R. van der Werf, and S. S. P. Shen (2009), Human amplification of drought-induced biomass burning in Indonesia since 1960, *Nat. Geosci.*, *2*, 185–188, doi:10.1038/ngeo443.
- Field, R. D., et al. (2016), Indonesian fire activity and smoke pollution in 2015 show persistent nonlinear sensitivity to El Niño-induced drought, *Proc. Natl. Acad. Sci. U.S.A.*, *113*, 9204–9209, doi:10.1073/pnas.1524888113.
- Glatthof, N., et al. (2015), Seasonal and interannual variations in HCN amounts in the upper troposphere and lower stratosphere observed by MIPAS, *Atmos. Chem. Phys.*, *15*, 563–582, doi:10.5194/acp-15-563-2015.
- Huijnen, V., M. J. Wooster, J. W. Kaiser, D. L. A. Gaveau, J. Flemming, M. Parrington, A. Inness, D. Murdiyarso, B. Main, and M. van Weele (2016), Fire carbon emissions over maritime southeast Asia in 2015 largest since 1997, *Sci. Rep.*, *6*, 26886, doi:10.1038/srep26886.
- Hsu, N. C., J. R. Herman, and S.-C. Tsay (2003), Radiative impacts from biomass burning in the presence of clouds during boreal spring in southeast Asia, *Geophys. Res. Lett.*, *30*(5), 1224, doi:10.1029/2002GL016485.
- Kaiser, J. W., et al. (2012), Biomass burning emissions estimated with a global fire assimilation system based on observed fire radiative power, *Biogeosciences*, *9*, 527–554, doi:10.5194/bg-9-527-2012.
- Li, Q., D. J. Jacob, R. M. Yantosca, C. L. Heald, H. B. Singh, M. Koike, Y. Zhao, G. W. Sachse, and D. G. Streets (2003), A global three-dimensional model analysis of the atmospheric budgets of HCN and CH₃CN: Constraints from aircraft and ground measurements, *J. Geophys. Res.*, *108*(D21), 8827, doi:10.1029/2002JD003075.
- Li, Q., P. I. Palmer, H. C. Pumphrey, P. Bernath, and E. Mahieu (2009), What drives the observed variability of HCN in the troposphere and lower stratosphere?, *Atmos. Chem. Phys.*, *9*, 8531–8543, doi:10.5194/acp-9-8531-2009.
- Park, M., W. J. Randel, D. E. Kinnison, L. K. Emmons, P. F. Bernath, K. A. Walker, C. D. Boone, and N. J. Livesey (2013), Hydrocarbons in the upper troposphere and lower stratosphere observed from ACE-FTS and comparisons with WACCM, *J. Geophys. Res. Atmos.*, *118*, 1964–1980, doi:10.1029/2012JD018327.
- Parker, R. J., H. Boesch, M. J. Wooster, D. P. Moore, A. J. Webb, D. Gaveau, and D. Murdiyarso (2016), Atmospheric CH₄ and CO₂ enhancements and biomass burning emission ratios derived from satellite observations of the 2015 Indonesian fire plumes, *Atmos. Chem. Phys.*, *16*, 10,111–10,131, doi:10.5194/acp-16-10111-2016.
- Pommrich, R., R. Müller, J.-U. Groöb, G. Günther, P. Konopka, M. Riese, A. Heil, M. Schultz, H.-C. Pumphrey, and K. A. Walker (2010), What causes the irregular cycle of the atmospheric tape recorder signal in HCN?, *Geophys. Res. Lett.*, *37*, L16805, doi:10.1029/2010GL044056.
- Pumphrey, H. C., C. Boone, K. A. Walker, P. Bernath, and N. J. Livesey (2008), Tropical tape recorder observed in HCN, *Geophys. Res. Lett.*, *35*, L05801, doi:10.1029/2007GL032137.
- Randel, W. J., M. Park, L. Emmons, D. Kinnison, P. Bernath, K. A. Walker, C. Boone, and H. Pumphrey (2010), Asian monsoon transport of pollution to the stratosphere, *Science*, *328*, 611–613, doi:10.1126/science.1182274.
- Rinsland, C. P., et al. (1999), Infrared solar spectroscopic measurements of free tropospheric CO, C₂H₆, and HCN above Mauna Loa, Hawaii: Seasonal variations and evidence for enhanced emissions from the Southeast Asian tropical fires of 1997–1998, *J. Geophys. Res.*, *104*, 18,667–18,680, doi:10.1029/1999JD900366.
- Rinsland, C. P., E. Mahieu, R. Zander, P. Demoulin, J. Forrer, and B. Buchmann (2000), Free tropospheric CO, C₂H₆, and HCN above central Europe: Recent measurements from the Jungfraujoch station including the detection of elevated columns during 1998, *J. Geophys. Res.*, *105*, 24,235–24,249, doi:10.1029/2000JD900371.
- Sheese, P. E., C. D. Boone, and K. A. Walker (2015), Detecting physically unrealistic outliers in ACE-FTS atmospheric measurements, *Atmos. Meas. Tech.*, *8*, 741–750, doi:10.5194/amt-8-741-2015.
- Singh, H. B., et al. (2003), In situ measurements of HCN and CH₃CN over the Pacific Ocean: Sources, sinks, and budgets, *J. Geophys. Res.*, *108*(D20), 8795, doi:10.1029/2002JD003006.
- van der Werf, G. R., J. T. Randerson, L. Giglio, G. J. Collatz, M. Mu, P. S. Kasibhatla, D. C. Morton, R. S. DeFries, Y. Jin, and T. T. van Leeuwen (2010), Global fire emissions and the contribution of deforestation, savanna, forest, agricultural, and peat fires (1997–2009), *Atmos. Chem. Phys.*, *10*, 11,707–11,735, doi:10.5194/acp-10-11707-2010.
- Viatte, C., K. Strong, K. A. Walker, and J. R. Drummond (2014), Five years of CO, HCN, C₂H₆, C₂H₂, CH₃OH, HCOOH and H₂CO total columns measured in the Canadian high Arctic, *Atmos. Meas. Tech.*, *7*, 1547–1570, doi:10.5194/amt-7-1547-2014.
- Wooster, M. J., G. Roberts, G. L. W. Perry, and Y. J. Kaufman (2005), Retrieval of biomass combustion rates and totals from fire radiative power observations: FRP derivation and calibration relationships between biomass consumption and fire radiative energy release, *J. Geophys. Res.*, *110*, D24311, doi:10.1029/2005JD006318.
- World Meteorological Organization (1957), *Meteorology: A Three-Dimensional Science: Second Session of the Commission for Aerology*, WMO Bull., vol. 4, pp. 134–138, WMO, Geneva, Switzerland.